FOUNDATIONS OF CIVIL AND ENVIRONMENTAL ENGINEERING

No. 7 2006

Zenon MRÓZ[1], Dariusz BOJCZUK[2*]
[1]Institute of Fundamental Technological Research, Warsaw, Poland
[2]Faculty of Management and Computer Modelling, University of Technology, Kielce, Poland

TOPOLOGICAL SENSITIVITY DERIVATIVE: APPLICATION IN OPTIMAL DESIGN AND MATERIAL SCIENCE

Received: 03 July 2006
Accepted: 01 September 2006

The concept of topological derivative is introduced and applied to optimal design of structural elements and to study the material microstructure evolution. For structural design the objective function and constraints provide the optimal design, for material microstructure the free energy and dissipation function generate the process of evolution such as phase transformation, crack growth or void generation. Three general modes of topology variation have been considered: generation of new elements, removing of the existing elements and a substitution of the existing elements by new elements. The cases of infinitesimal and finite topology variations have been discussed and illustrated by examples.

Key words: topological derivative, finite topology variation, structure and material evolution, optimal topology and shape

1. INTRODUCTION

The problems of optimal design taking the account of topology modification have recently been studied for both material and structural elements. For a material element the topology variation corresponds to the introduction of voids, inclusions, cracks, nucleation of different crystalline phases, etc. For a structure

* Corresponding author. Tel.: 0048-41-3424-363; fax: 0048-41-3424-306.
E-mail address: mecdb@eden.tu.kielce.pl (D. Bojczuk)

ISSN 1642-9303

the topology variation corresponds to the introduction or removing of members, connecting nodes, supports etc., and to the replacement of the existing elements by new elements.

The uniform treatment of topology and shape optimization for a material element can be obtained by assuming a microstructure with its parameters optimized at the element level, for instance, by homogenization technique and with the spatial evolution of microstructure generated by a global solution for the whole structure. A simplified approach of this type is based on the artificial density distribution specifying the microstructure evolution in terms of one scalar variable, cf. [1], [2], [3]. The stiffness moduli are assumed to be proportional to the relative material density raised to some power. A number of numerical schemes have been developed within the homogenization method using the penalization of intermediate densities (SIMP-method). An alternative approach such as bubble method proposed in [13], generates the topology variation by the introduction of voids into the structure domain with subsequent optimization of their position, size and shape. An alternative variant of this method was presented in [27], where the concept of gradual removal of the material in order to obtain the optimal design is used. This approach based on evolutionary strategy (ESO) proved efficient in effective redesign of structural elements. The concept of virtual topology variation and topological sensitivity derivative for truss and beam structures was introduced in [5], [6], [7], [19] by specifying a class of admissible topologies in the redesign process. The optimal support and loading conditions were considered in [14] and [21]. The topological sensitivity derivative provides the gradients of objective function and constraints with respect to topology parameters. This derivative provides the conditions for the acceptance or rejection of a new topology. Once a new topological structure is accepted, the usual shape and material optimization is performed in order to determine the optimal configuration, the cross-sectional and material parameters. The case of void generation in an elastic material was studied in [24], where analytical expressions for the topological sensitivity derivative were derived. The evolutionary algorithms combined with the boundary element method were developed in [9] and applied in topology and shape optimization. The review of optimal topology design of truss or plate structures was provided in [16].

The combined shape and topology optimization was recently developed by applying the level-set-based method originally devised in [23] for numerical analysis of evolving interfaces, cf. [25] and [26]. In fact, the shape sensitivity for an assumed integral of state fields is expressed in terms of boundary energy or mutual energy of primary and adjoint states, cf. [11] or [22]. The optimality conditions then require uniform values of generalized energy on the varying boundary. In the level-set method, the structure boundary is assumed to coincide with the iso-values of the assumed scalar function Φ representing the generalized energy with higher values within the structure domain and lower values in its

its exterior. The generation of voids is then naturally induced in domains of lower values of Φ than the assumed design value.

In the next section we shall discuss the concept of topological derivative and the associated optimality conditions. The implications in material science are discussed in Section 3. In Section 4 problems of topology, shape and reinforcement optimization of disk and plate structures are discussed and illustrated by simple examples.

2. TOPOLOGICAL SENSITIVITY DERIVATIVE AND ITS APPLICATION

In structural design problems, we usually introduce different classes of parameters, such as material parameters η_m, size parameters η_d, (such as length L_e, area A_e, volume V_e or mass M_e), shape parameters η_s, orientation and position parameters η_α. Let us assume that we introduce a new element in the structure, such as void, crack or inclusion of a specified shape. In beam or plate structures this element may be represented by introduced bar, segment, or stiffener. Consider a global state functional $\Pi = \Pi(\boldsymbol{\varepsilon}, \mathbf{u}, \eta_m, \eta_d, \eta_s, \eta_\alpha)$ such as a potential or complementary energy, mutual energy of two states, etc. The topological derivative specifies the variation of Π with respect to the size parameter assuming the shape parameters as fixed. We have the topological derivatives

$$T_{,A}^{\Pi} = \left(\frac{\delta \Pi}{\delta A_e}\right)_{A_e=0}, \qquad T_{,V}^{\Pi} = \left(\frac{\delta \Pi}{\delta V_e}\right)_{V_e=0}, \qquad T_{,L}^{\Pi} = \left(\frac{\delta \Pi}{\delta L_e}\right)_{L_e=0}. \tag{2.1}$$

These derivatives specified at vanishing size parameters depend on shape parameters of the void or inclusion. To illustrate this dependence, consider an example of an elliptical cavity in a plane sheet loaded biaxially by the principal stresses σ_1, σ_2 oriented along the principal ellipse axes, Fig. 1. The increment of sheet compliance S_c measured by the release of potential energy Π due to void presence is expressed as follows for the plane strain condition

$$\begin{aligned} \Delta S_c = -\Delta \Pi &= \frac{\pi(1-\nu^2)}{E}\left[\sigma_2^2 a^2 + \sigma_1 b^2 + \tfrac{1}{2}(\sigma_1 - \sigma_2)^2 a\, b\right] = \\ &= \frac{1-\nu^2}{E} A\left[\sigma_2^2 \frac{1}{\eta} + \sigma_1^2 \eta + \tfrac{1}{2}(\sigma_1 - \sigma_2)^2\right], \end{aligned} \tag{2.2}$$

where E, ν denote the elastic moduli, $A = \pi ab$ is the ellipse area and $\eta = b/a$ is the shape parameter. The topological derivative now equals

$$T_{,A}^{\Pi} = -\left(\frac{\delta \Pi}{\delta A}\right)_{A=0} = \frac{1-\nu^2}{E}\left[\sigma_2^2 \frac{1}{\eta} + \sigma_1^2 \eta + \tfrac{1}{2}(\sigma_1 - \sigma_2)^2\right]. \tag{2.3}$$

From (2.3) it follows that for the specific cases we have:

i) for $\eta = \dfrac{b}{a} = 0$, $\quad b = 0$, $\quad T_{,A}^{\Pi} = \infty$, $\qquad$ crack

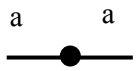

(crack along x–axis);

ii) for $\eta = \dfrac{b}{a} = \infty$, $\quad a = 0$, $\quad T_{,A}^{\Pi} = \infty$, $\qquad$ crack

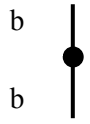

(crack along y–axis);

iii) for $\eta = \dfrac{b}{a} = 1$, $\quad T_{,A}^{\Pi} = \dfrac{1-\nu^2}{E}\left[\dfrac{3}{2}\left(\sigma_1^2 + \sigma_2^2\right) - \sigma_1 \sigma_2\right]$, $\qquad$ void

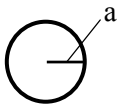

(circular cavity of radius $a = b$).

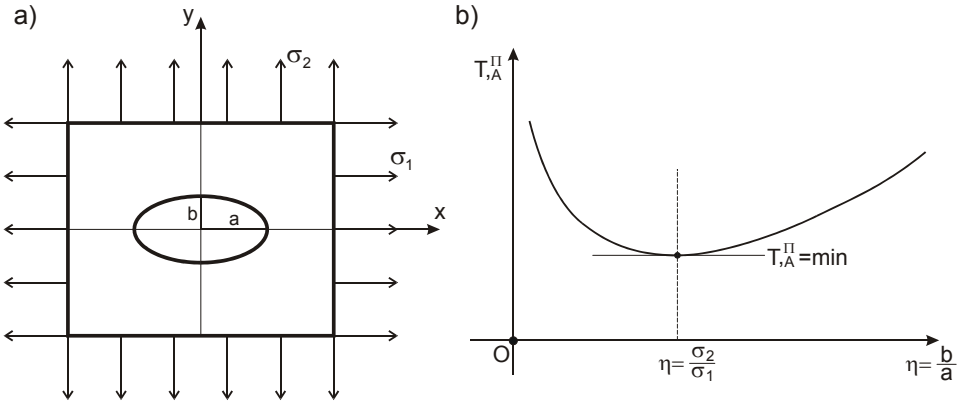

Fig. 1. Biaxially loaded plane sheet: a) introduction of elliptical cavity, b) dependence of the topological sensitivity derivative on a shape parameter η

The minimum of the topological derivative can be specified from (2.3), thus

$$\frac{\partial T_{,A}^{\Pi}}{\partial \eta} = 0 \quad \text{for} \quad \eta = \frac{\sigma_2}{\sigma_1}, \quad \text{and} \quad \left(T_{,A}^{\Pi}\right)_{\min} = \frac{1-\nu^2}{E}(\sigma_1 + \sigma_2)^2. \tag{2.4}$$

From (2.3) it follows that the topological derivative depends on the cavity shape, reaching infinite values for $\eta = 0$ and $\eta = \infty$ (cracks) and a minimum for the specific value $\eta = \sigma_2/\sigma_1$. In fact, this ratio specifies the optimal cavity shape for the prescribed stress biaxiality. Further, for the case of crack, there exists a topological derivative with respect to crack length. Setting successively $b = 0$ and $a = 0$ in (2.2) we obtain

$$b=0:\ T^{\Pi}_{,a} = 2\frac{\pi\left(1-\nu^2\right)}{E}\sigma_2^2 a\,, \qquad a=0:\ T^{\Pi}_{,b} = 2\frac{\pi\left(1-\nu^2\right)}{E}\sigma_1^2 b \tag{2.5}$$

and the topological derivatives grow linearly with the crack length. The topological derivatives associated with an arbitrary state functional and generation of spherical or circular cavities were derived in [24] and [8], and expressed in terms of primary and adjoint states.

Consider now a more general case of introduction of a new topological structure within the design domain, such as an inclusion (or bar and stiffener). Assume this structure as an element of volume V_e and parameters p_l $(l = 1, 2, ..., s)$ specifying its shape, orientation and material properties. Assume the potential energy Π of the structure to grow linearly with V_e, so that

$$\Delta\Pi = V_e U\left(\boldsymbol{\varepsilon}, p_l\right), \tag{2.6}$$

where $\boldsymbol{\varepsilon}$ is the strain state within the element. Assume the cost function to be a non-linear function of V_e, composed of the installation cost C_i and the material cost C_m, so that

$$C = C_i\left(V_e\right) + C_m\left(V_e\right) = C\left(V_e\right)\,, \tag{2.7}$$

where $C_i\left(V_e\right)$ grows non-linearly with V_e and $C_m\left(V_e\right)$ depends linearly on V_e, Fig. 2. Consider the problem of maximization of the global structure stiffness with constraint set on the element cost, so that we have

$$\max\ \ \Delta\Pi\left(V_e, \boldsymbol{\varepsilon}, p_l\right) \quad \text{subject to} \quad C - C_0 \le 0\ . \tag{2.8}$$

Introducing the Lagrangian $L = \Delta\Pi - \lambda\left(C - C_0\right)$, where $\lambda \ge 0$, the optimality conditions provide

$$\frac{\partial\left(\Delta\Pi\right)}{\partial V_e} - \lambda\frac{\partial C}{\partial V_e} = U_e - \lambda\frac{\partial C}{\partial V_e} = 0\,, \qquad \frac{\partial\left(\Delta\Pi\right)}{\partial p_l} = 0\,. \tag{2.9}$$

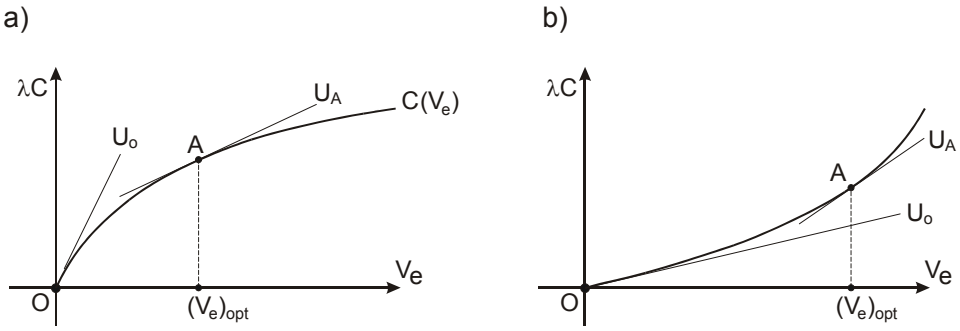

Fig. 2. Non-linear cost function: optimality conditions at points A and O: a) concave cost function, b) convex cost function

Fig. 2 illustrates the optimality condition (2.9). The gradient of the potential energy equals $U(\boldsymbol{\varepsilon}, p_l)$, thus, the straight line of this slope should be tangent to the cost function $\lambda\, C(V_e)$. This specifies point A and also the volume (and size) of the inclusion, Fig. 2a. On the other hand, when the inclusion of vanishing volume $V_e = 0$ is introduced, the line of slope U_0 is tangent to the cost function at the point O. Assuming $U(\boldsymbol{\varepsilon}, p_l)$ to be a monotonic (quadratic) function of $\boldsymbol{\varepsilon}$, it is seen that for the concave cost function the optimality condition at O occurs at larger strain than at A, Fig. 2a. On the other hand, for a convex cost function, Fig. 2b, the generation of inclusion of vanishing size at the point O occurs at lower strain value as compared to a finite size inclusion corresponding to the point A. So, for a concave cost function, the nucleation of inclusion requires a higher specific energy and stress or strain levels than the generation of inclusion of the finite size. This means that for an increasing stress induced by loading the generated inclusion must be of finite size. We shall call this case the *finite topology transformation*. On the other hand, for the convex cost function, the inclusion is generated from its initial vanishing size and grows consecutively for increasing stress levels. We shall call this case the *infinitesimal topology variation*. We have

$$\left.\frac{\partial \Pi}{\partial V_e}\right|_{V_e=0} = U_0(\boldsymbol{\varepsilon}, p_l), \qquad \left.\frac{\partial C}{\partial V_e}\right|_{V_e=0} = C'(0), \tag{2.10}$$

and the optimality condition provides

$$U_0 = \lambda\, C'(0). \tag{2.11}$$

The next step would require the maximization of $\Delta\Pi$ with respect to the configuration and cross sectional parameters p_l with the optimality conditions (2.9).

The problem of material or element replacement can be formulated in terms of the concept of finite topological transformation. Let us assume that the material volume V_e is removed from the location 1 and placed at the location 2 of a higher strain energy. The optimality condition now provides

$$U(\boldsymbol{\varepsilon}_2, p_l) - U(\boldsymbol{\varepsilon}_1, p_l) = \lambda\ C_i(V_e), \tag{2.12}$$

where $\boldsymbol{\varepsilon}_2$ and $\boldsymbol{\varepsilon}_1$ denote the strain states at locations 2 and 1. A similar condition applies when two material elements are exchanged between the locations 1 and 2.

The case of discontinuous cost function can be treated assuming a finite topology transformation. Assume that

$$C = C_i + c_m V_e\ , \tag{2.13}$$

where C_i is constant. Introducing the Lagrangian

$$L = U(\varepsilon)V_e - \lambda(C_i + c_m V_e)\ , \tag{2.14}$$

assume that a finite transformation corresponds to the balance of global stiffness increase and cost. Setting $L = 0$, we obtain

$$V_e = \frac{\lambda C_i}{U(\varepsilon) - \lambda c_m}\ , \qquad U(\varepsilon) - \lambda c_m > 0\ . \tag{2.15}$$

The first equation provides the volume (size) of an element, the inequality provides the condition for the generation of a rotation new element.

3. APPLICATION IN MATERIAL SCIENCE: NUCLEATION AND GROWTH

The concept of topological sensitivity derivative discussed in the previous section can now be applied in material science, namely to the process of nucleation and growth of new phases, such as nucleation of a liquid from the vapour, solidification, phase transformation (such as austenite – martensite in carbon steels), recrystallization, crack generation, etc. The new phase usually, generates

as a volume or plane element of a finite size and then grows in a kinetic process, cf. [15].

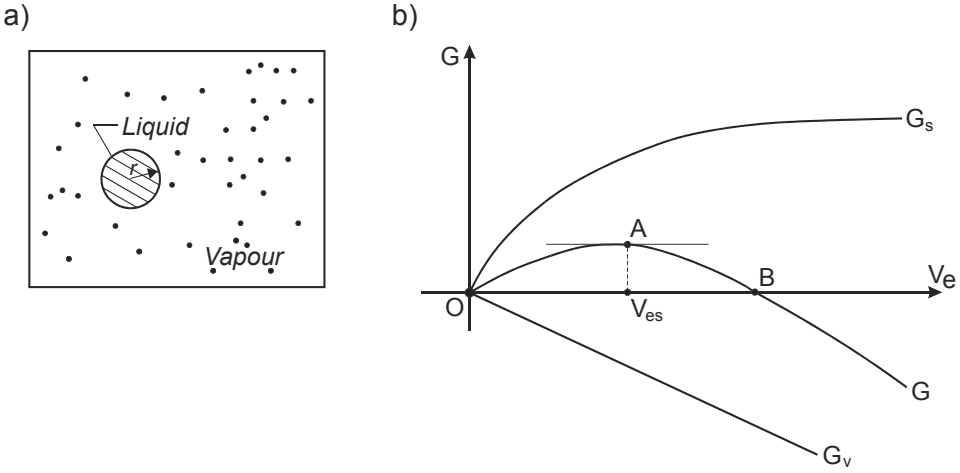

Fig. 3. Nucleation of liquid droplets from a vapour: a) spherical droplet, b) variation of free energy with droplet size

Consider the simplest process of liquid droplet formation in a vapour phase, Fig. 3. Assume the free energy associated with the formation of droplet in the form

$$\Delta G = \Delta G_V + \Delta G_s = -\alpha\, V_e + \gamma V_e^{2/3} = -\alpha V_e + \gamma S\,, \tag{3.1}$$

where $V_e = \frac{4}{3}\pi r^3$, $S = 4\pi r^2$ denote the volume and surface of the droplet, α denotes the difference of specific free energies of vapour and liquid and γ is the specific surface energy of the droplet. Fig. 3b presents the variation of free energies with the droplet volume. From the stationary condition we obtain

$$V_{es} = \frac{4}{3}\pi r_s^3 = \left(\frac{2}{3}\,\frac{\gamma}{\alpha}\right)^3, \qquad r_s = \frac{2}{3}\,\frac{\gamma}{\alpha}\left(\frac{3}{4\pi}\right)^{\frac{1}{3}}, \tag{3.2}$$

that is the critical size specifying stable droplet configuration. In fact, droplets of radius $r < r_s$ cannot nucleate, as it would increase the free energy with respect to the vapour free energy.

The nucleation of solid polycrystalline grain is more complex since there is interaction between size and shape dependence of free energy, but the finite size is a natural effect of new phase generation.

Instead of deriving the stable size of droplet, we may also consider a transformation at the same energy level, namely a finite transformation from vapour phase to droplet phase at G = const (that is from point O to point B in Fig. 3b). We have a condition

$$\Delta G = -\alpha V_e + \gamma V_e^{2/3} = 0, \quad \text{and} \quad V_e = \left(\frac{\gamma}{\alpha}\right)^3, \tag{3.3}$$

which provides larger value of the droplet radius.

The other example is associated with the crack nucleation process. It is well known that in Griffith theory the existence of cracks of length (or diameter) $2a$ in material or structure is assumed. However, the nucleation would require infinite stress values, contrary to general observations. Fig. 4 presents the potential energy variation dependent on the crack length.

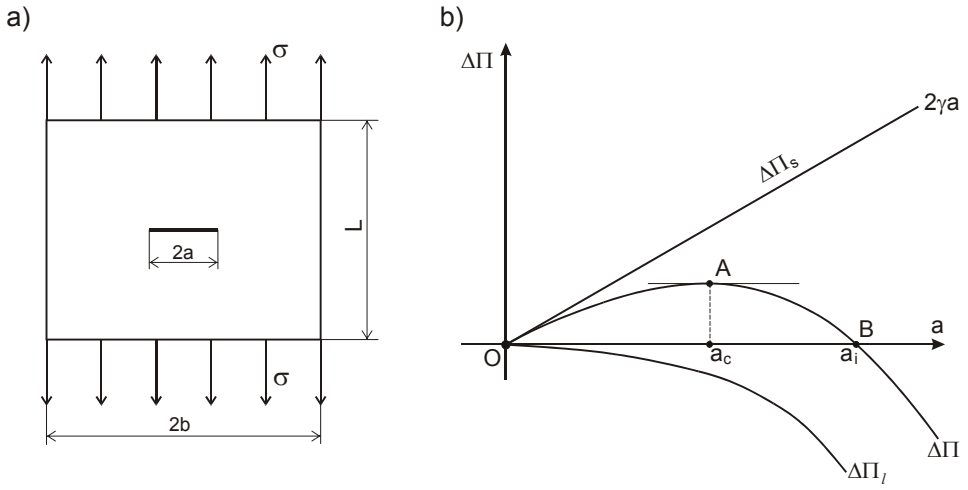

Fig. 4. Plane crack under tensile stress: a) element and crack dimensions, b) potential energy and dissipation variation

For a wide plate loaded uniaxially we have, Fig. 4a

$$\Delta\Pi = \Delta\Pi_l + \Delta\Pi_s = \frac{-\pi a^2 \sigma^2}{E} + 2\gamma a, \tag{3.4}$$

where $\Delta\Pi_l$ denotes the potential energy release due to crack presence and $\Delta\Pi_s = 2\gamma a$ represents the surface energy or the dissipated energy in the process of crack growth. The critical crack length is specified by the condition

$$\frac{\partial(\Delta\Pi)}{\partial a}=0, \quad \text{where } a_c=\frac{\gamma E}{\pi\sigma^2}\ , \tag{3.5}$$

and for $a > a_c$ there is unstable crack growth at constant stress with associated decrease of the free energy. The constant energy transformation now corresponds to $\Delta\Pi = 0$ and

$$a_i=\frac{2\gamma E}{\pi\sigma^2}\,. \tag{3.6}$$

The topological transformation occurs along the path OB, Fig. 4b. The concept of finite crack generation can be used in deriving the rupture stress of an element. Consider a plane element of length L, width $2b$ and unit thickness under uniaxial stress σ. Assume that at the critical stress value $\sigma = \sigma_c$ the element breaks into two pieces, with the crack length $2a = 2b$. Assuming $\Delta\Pi = 0$, we have

$$\frac{1}{2}\frac{\sigma_c^2}{E}2bL=2b\gamma \tag{3.7}$$

and

$$\sigma_c=\sqrt{\frac{2E\gamma}{L}}\ . \tag{3.8}$$

Thus the critical stress will increase for decreasing length of the element.

The present discussion exhibits the general concept of topology transformation in material science and optimal design. The objective and cost functions specify the problem types of optimal design. In material structure the free energy and the dissipation functions play a similar role. These two research areas should interact to develop general methodology in the analysis and optimization of material structures.

4. OPTIMAL DESIGN OF DISK AND PLATE STRUCTURES

The concept of topological derivative can be applied in optimization of disk and plate structures. In this Section the problem of optimal topology and shape design and the problem of optimal reinforcement are discussed.

4.1. Optimal design of topology and shape

Consider a general optimization problem of the form

$$\min G, \quad \text{subject to} \quad C - C_0 \le 0, \tag{4.1}$$

where G is the objective functional (function), C denotes the global cost and C_0 is the upper bound on the global cost. When $G = -\Delta\Pi$ it corresponds to the problem (2.8). Introducing the Lagrangian $L = G + \lambda(C - C_0)$, where $\lambda \ge 0$, the optimality conditions with respect to shape and dimensional parameters, can be presented in the form analogous to (2.9). The optimal values of these design parameters and of Lagrange's multiplier λ can be determined in the incremental process of gradient optimization.

Then, we try to introduce topology modification. The condition of introduction of an infinitesimally small circular hole of area A_0 at the arbitrary point **x**, using the concept of topological derivative, takes the form

$$T^L_{,A_0}(\mathbf{x}) = T^G_{,A_0}(\mathbf{x}) + \lambda T^C_{,A_0}(\mathbf{x}) < 0, \tag{4.2}$$

where $T^L_{,A_0}(\mathbf{x})$, $T^G_{,A_0}(\mathbf{x})$, $T^C_{,A_0}(\mathbf{x})$ are the topological derivatives, respectively of the Lagrangian, the objective functional G and the cost functional C. Moreover, a new small hole should be introduced at a point, where $T^L_{,A_0}(\mathbf{x})$ reaches the minimum value (cf. bubble method [13]).

However, in order to accelerate the optimization process, finite modifications can be applied. Here, the approach presented in [8] is used. Now, the problem consists in introduction of finite holes of an unknown size and shape together with the introduction of finite changes of other boundaries. It is assumed, that domains of relatively small values of the topological derivative of the Lagrangian, which is expressed by (4.2), should be removed. As for the redesign path related to the constant cost C_0 and minimum of the objective function G, the multiplier λ achieves its minimum at the optimal point, then for the finite variations of the design we can introduce the design quality function Λ (cf. [20]). Now, assuming that for a redesign process considered here $\Delta C < 0$, the preliminary problem can be presented as follows

$$\min_A \Lambda, \quad \text{where} \quad \Lambda = \frac{\mu\lambda + \Delta G}{\mu - \Delta C} = \frac{\mu\lambda + \int_A T^G_{,A_0}(\mathbf{x})dA}{\mu - \int_A T^C_{,A_0}(\mathbf{x})dA}, \tag{4.3}$$

while the condition of acceptance of the finite topology modification takes the form

$$\Lambda < \lambda. \tag{4.4}$$

Here, A denotes the unknown area of the hole and μ ($\mu \geq 0$) is the scaling factor controlling amount of the removed domain. When μ tends to infinity, the whole domain for which $\lambda > -\dfrac{\delta G}{\delta C}$ will be removed. On the other hand, when $\mu = 0$, the condition (4.4) related with the problem (4.3) becomes analogous to the condition (4.2) and corresponds to introduction of infinitesimally small holes.

After finite topology modifications only an improved structure is obtained, so additional standard shape and dimensional optimization should be done.

In order to perform this optimization process we need topological derivatives of the objective functional G and the constraints with respect to the introduction of infinitesimally small circular hole. Here, the expressions for topological derivatives, which were derived in [8] and [24] using adjoint method, are presented.

Let $A \subset R^2$, be a domain occupied by an elastic disk with a boundary $\Gamma = \Gamma_u \cup \Gamma_T$. It is subjected to surface traction $\mathbf{T}^0$ on Γ_T and on boundary Γ_u displacements $\mathbf{u}^0$ are given. Consider for example a functional of strain $\boldsymbol{\varepsilon}$ and displacement $\mathbf{u}$ in the form

$$G = \int_A F(\boldsymbol{\varepsilon})\, dA + \int_{\Gamma_T} f(\mathbf{u})\, d\Gamma_T \ . \tag{4.5}$$

Introduce now an adjoint structure of the same shape as the primary structure, but subjected to initial generalized stresses $\mathbf{N}^{ai} = \boldsymbol{\sigma}^{ai} h$, namely

$$\mathbf{N}^{ai} = \frac{\partial F}{\partial \boldsymbol{\varepsilon}} \quad \text{in } A, \tag{4.6}$$

where $\boldsymbol{\sigma}^{ai}$ is the corresponding initial stresses and h is the thickness of the disk. The field of the initial generalized stresses induces the field of the global generalized stresses $\mathbf{N}^a = \mathbf{N}^{ai} + \mathbf{N}^{ar}$, where $\mathbf{N}^{ar}$ is the field of the elastic generalized stresses. The boundary conditions are assumed as follows

$$\mathbf{T}^{a0} = \mathbf{0} \text{ on } \Gamma_T, \quad \mathbf{u}^{a0} = \mathbf{0} \text{ on } \Gamma_u \, . \tag{4.7}$$

Finally (cf. [8]), the topological derivative of the functional (4.5) takes the form

$$T^G_{,A_0}(\mathbf{x}) = h\left[\frac{1}{E}(\sigma_1 + \sigma_2)(\sigma_1^a + \sigma_2^a) + \frac{2}{E}(\sigma_1 - \sigma_2)(\sigma_1^a - \sigma_2^a)\cos 2\alpha + \right. \\ \left. - F_0\right], \tag{4.8}$$

where σ_1, σ_2, σ_1^a, σ_2^a are the principal stresses at the considered point, respectively for the primary and adjoint structures, and α is the angle between corresponding principal directions. Here, all quantities are calculated at the point $\mathbf{x}$ and the expression $F_0 = \frac{1}{2\pi}\int_0^{2\pi} \mathrm{F}\, d\theta$ should be determined separately for each form of the function F. In the case of the strain energy U, the adjoint structure is the same as the primary one and (4.8) becomes

$$T^G_{,A_0}(\mathbf{x}) = \frac{h}{2E}\left[(\sigma_1+\sigma_2)^2 + 2(\sigma_1-\sigma_2)^2\right]. \tag{4.9}$$

Next, consider a flexural plate whose middle surface occupies the domain $A \subset R^2$, with a boundary Γ. The plate is subjected to a transverse load $\mathbf{p}^0$ in A, whereas either generalized traction $\mathbf{T}^0$ or displacements are specified on Γ. Here, Kirchhoff's theory of thin plates is used. Consider a case when the functional of curvatures $\boldsymbol{\kappa}$ and transverse displacements w is of the form

$$G = \int_A F(\boldsymbol{\kappa})\, dA + \int_A f(w)\, dA. \tag{4.10}$$

In this case the adjoint structure is subjected to initial bending moments $\mathbf{M}^{ai}$, and transverse load p^{a0}, namely

$$\mathbf{M}^{ai} = \frac{\partial F}{\partial \boldsymbol{\kappa}} \ \text{ in } A, \quad p^{a0} = \frac{\partial f}{\partial w} \ \text{ in } A. \tag{4.11}$$

Furthermore, we assume that on the boundary Γ the adjoint plate is supported in the same way as the primary one. The field of the initial moments $\mathbf{M}^{ai}$ induces field of the global moments $\mathbf{M}^a = \mathbf{M}^{ai} + \mathbf{M}^{ar}$, where $\mathbf{M}^{ar}$ is the field of elastic moments. Finally (cf. [8]), the topological derivative of the functional (4.10) takes the form

$$\begin{aligned} T^G_{,A_0}(\mathbf{x}) &= \frac{12}{Eh^3}\left[(M_1+M_2)(M_1^a+M_2^a) + 2(M_1-M_2)(M_1^a-M_2^a)\cos 2\alpha\right] + \\ &- \int_{-h/2}^{h/2} F_0\, dx_3 - f - p^0 w^a, \end{aligned} \tag{4.12}$$

where M_1, M_2, M_1^a, M_2^a are the principal moments at the point $\mathbf{x}$, respectively for the primary and adjoint structures, and α is the angle between corre-

sponding principal directions. Moreover, F_0 is defined in the same way as in (4.8), x_3 denotes axis normal to the middle surface and h is the thickness of the plate. When G coincides with the strain energy, and $f = 0$, $p^0 = 0$ on boundary Γ_ρ of a new hole, the topological derivative reduces to the form

$$T^G_{,A_0}(\mathbf{x}) = \frac{6}{Eh^3}\left[(M_1 + M_2)^2 + 2(M_1 - M_2)^2\right]. \tag{4.13}$$

The formulas for the topological derivatives of cost functionals and functionals of stresses and reactions can be found in [8].

4.2. Example: optimization of topology and shape of a plane beam–like structure

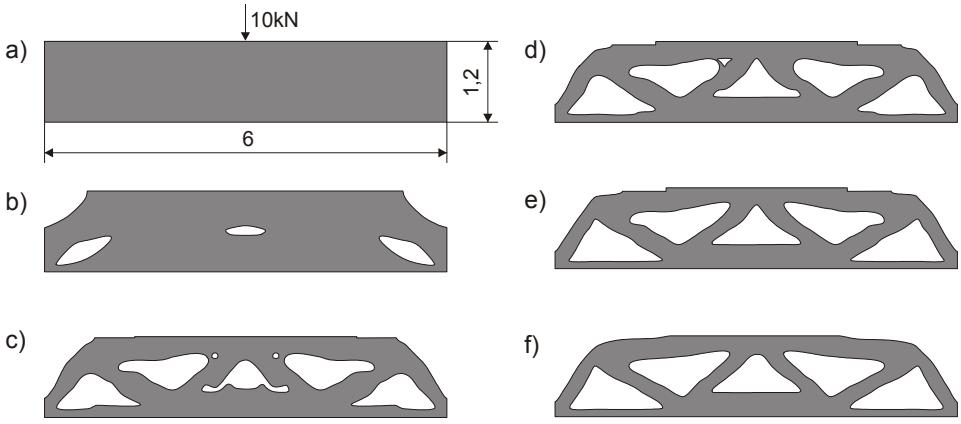

Fig. 5. History of optimization of a plane beam-like structure: a) initial structure, b)÷e) succesive finite modifications, f) final design

Let us consider an optimal design problem (4.1) for the plane structure shown in Fig. 5a, where G corresponds to the global strain energy U and the cost C is proportional to the global material volume (cf. [8]). The structure is made of steel, where the Young modulus $E = 2.1 \cdot 10^5$ MPa and the Poisson's ratio $\nu = 0.3$. The initial structure domain is divided into 2880 finite elements. The structure is simply supported at end points of the lower boundary and loaded by a concentrated force F = 10kN at the mid-point of the upper boundary, Fig. 5a.

The history of optimization is shown in Fig. 5. The optimal structure, presented in Fig. 5f, is obtained after 5 finite modifications and final correction of

the shape. The ratio of the strain energies of the initial and optimal designs is $U^{(init)}/U^{(opt)} = 1.275$.

4.3. Optimal design of reinforcement

The problem of optimal reinforcement was previously analyzed in [10], [12], [17]. In this subsection the problem of optimal reinforcement of disks and bending Kirchhoff plates is discussed in view of results presented in [4]. Two types of reinforcement are considered here, namely the introduction of fibers into disks and introduction of ribs into plates. The optimization problem of the form (4.1) is considered. In order to find optimal reinforcement, a heuristic algorithm has been proposed in the paper. At first, using topological derivative, an initial location of a new fiber or a rib is determined. Next, in order to correct their positions and to determine other parameters characterizing stiffened structure, the standard optimization procedure is performed. Usually, the optimal position of the stiffener differs insignificantly from its initial position.

Now, using the adjoint structure method, the respective formulas for the topological derivatives of the assumed functionals of strains, curvatures and displacements, expressed by (4.5) and (4.10), will be provided.

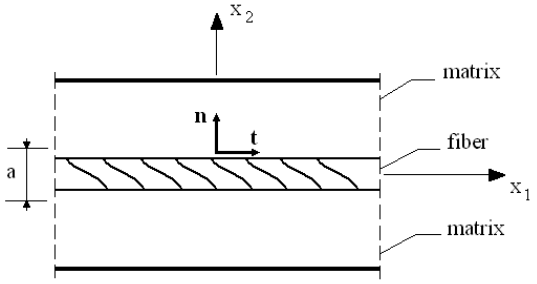

Fig. 6. Geometry of the disk reinforced by the fiber

Consider, similarly to Subsection 4.1, an elastic disk, but made of fibrous composite, which can be treated as an orthotropic material (Fig. 6). Now, the stress–strain relation in the principal directions of orthotropy can be written as follows

$$\boldsymbol{\sigma} = \mathbf{Q}^0 \boldsymbol{\varepsilon}, \tag{4.14}$$

where $\mathbf{Q}^0$ is the reduced stiffness matrix. Assume that on the interface S_C separating domains of different materials properties, we have

$$[\mathbf{u}] = \mathbf{0}, \quad [\varepsilon_{11}] = [\varepsilon_{tt}] = 0, \quad [\sigma_{22}] = [\sigma_{nn}] = 0, \quad [\sigma_{21}] = [\sigma_{nt}] = 0, \tag{4.15}$$

where $[\ ]$ denotes the jump of the enclosed quantity on S_C calculated as a difference of the respective values in the matrix and in the fiber. Moreover, *n*, *t* are the directions normal and tangential to S_C. The values of the 'reduced stiffnesses' Q_{11}^0, Q_{12}^0, Q_{22}^0, Q_{66}^0 in terms of engineering constants E_1, E_2, ν_{12}, G_{12} are

$$\begin{aligned} Q_{11}^0 &= \frac{E_1}{1-\nu_{12}\nu_{21}}, & Q_{12}^0 = Q_{21}^0 &= \frac{\nu_{12}E_2}{1-\nu_{12}\nu_{21}} = \frac{\nu_{21}E_1}{1-\nu_{12}\nu_{21}}, \\ Q_{22}^0 &= \frac{E_2}{1-\nu_{12}\nu_{21}}, & Q_{66}^0 &= G_{12}\,. \end{aligned} \tag{4.16}$$

The engineering constants of a composite, in view of (4.15), can be determined by using the rule of mixtures (cf. [18]), namely

$$\begin{aligned} E_1 &= V_f E_f + V_m E_m\,, & E_2 &= \frac{E_f E_m}{V_m E_f + V_f E_m}, \\ \nu_{12} &= V_f \nu_f + V_m \nu_m\,,\ \ \nu_{21} = \frac{E_2}{E_1}\nu_{12}\,, & G_{12} &= \frac{G_f G_m}{V_m G_f + V_f G_m}, \end{aligned} \tag{4.17}$$

where ν_f, ν_m, E_f, E_m, G_f, G_m are the Poisson's ratios, Young and Kirchhoff moduli, respectively for the fiber and matrix materials. Moreover, V_f, V_m denote the non-dimensional, volumetric fiber and the matrix fractions, $\left(V_f + V_m = 1\right)$.

Consider now the functional (4.5) of strains and displacements and assume the non-dimensional, volumetric fiber concentration V_f as the topological parameter. The topological derivative should be determined at the point corresponding to zero concentration of fibers i.e. $V_f = 0$. So, using the adjoint method, where adjoint structure is defined by (4.6), (4.7), the topological derivative takes the form (cf. [4])

$$\begin{aligned} \left.\frac{\partial G}{\partial V_f}\right|_{V_f=0} = a\int_l \Bigg[& \left.\frac{\partial F}{\partial V_f}\right|_{V_f=0} - h\varepsilon_{11}\varepsilon_{11}^a \left.\frac{\partial Q_{11}^0}{\partial V_f}\right|_{V_f=0} - h\varepsilon_{22}\varepsilon_{22}^a \left.\frac{\partial Q_{22}^0}{\partial V_f}\right|_{V_f=0} + \\ & - h\left(\varepsilon_{11}\varepsilon_{22}^a + \varepsilon_{22}\varepsilon_{11}^a\right)\left.\frac{\partial Q_{12}^0}{\partial V_f}\right|_{V_f=0} - 4h\varepsilon_{12}\varepsilon_{12}^a \left.\frac{\partial Q_{66}^0}{\partial V_f}\right|_{V_f=0} \Bigg] dl\,, \end{aligned} \tag{4.18}$$

where the integral is calculated along the line l corresponding to the position of new fiber, while a denotes width of the domain cooperating with the fiber (Fig. 6). This domain was assumed, to be of small dimension. Moreover, derivatives of particular components of the reduced stiffness matrix $\mathbf{Q}^0$ at the point $V_f = 0$, in view of (4.16) and (4.17), are equal to

$$\begin{aligned}
&\left.\frac{\partial Q_{11}^0}{\partial V_f}\right|_{V_f=0} = \frac{\left(E_f - E_m\right)E_f + B}{E_f\left(1-\nu_m^2\right)},\\
&\left.\frac{\partial Q_{22}^0}{\partial V_f}\right|_{V_f=0} = \frac{\left(E_f - E_m\right)E_m + B}{E_f\left(1-\nu_m^2\right)},\\
&\left.\frac{\partial Q_{12}^0}{\partial V_f}\right|_{V_f=0} = \frac{\left(E_f - E_m\right)E_m\nu_m + B\nu_m + E_m E_f\left(\nu_f - \nu_m\right)}{E_f\left(1-\nu_m^2\right)},\\
&\left.\frac{\partial Q_{66}^0}{\partial V_f}\right|_{V_f=0} = \frac{\left(G_f - G_m\right)G_m}{G_f} = \left[1 - \frac{E_m\left(1+\nu_f\right)}{E_f\left(1+\nu_m\right)}\right]\frac{E_m}{2\left(1+\nu_m\right)},
\end{aligned} \tag{4.19}$$

where $B = \dfrac{\nu_m}{1-\nu_m^2}\left[2E_f E_m\nu_f - \left(E_m^2 + E_f^2\right)\nu_m\right]$.

Consider now, similarly as in Subsection 4.1, an elastic plate. It is made of an isotropic material, but after the introduction of a rib it behaves as the orthotropic structure. Now, the constitutive relation in the principal directions of orthotropy can be written as follows

$$\mathbf{M} = \mathbf{D}^0\boldsymbol{\kappa}, \tag{4.20}$$

where $\mathbf{D}^0$ is the stiffness matrix. Assume that on the interface S_C separating rib and remaining part of the plate, the continuity conditions are of the form

$$[w] = 0, \quad [\kappa_{11}] = [\kappa_{tt}] = 0, \quad [M_{22}] = [M_{nn}] = 0, \quad [M_{21}] = [M_{nt}] = 0, \tag{4.21}$$

where the last condition sometimes is assumed in the form $[\kappa_{21}] = [\kappa_{nt}] = 0$, or in the mixed form. Now, using the homogenization theory, (cf. [18]), the averaged stiffness moduli of the plate in the domain cooperating with the rib, specified by dimension a (Fig. 7), take the form

$$
\begin{aligned}
D_{11}^0 &= \frac{E}{12}\frac{a_1 h_1^3 + a_2 h_3^3}{a} + \frac{E\nu^2}{12\left(1-\nu^2\right)}\frac{a}{\dfrac{a_1}{h_1^3}+\dfrac{a_2}{h_3^3}}, \\
D_{22}^0 &= \frac{E}{12\left(1-\nu^2\right)}\frac{a}{\dfrac{a_1}{h_1^3}+\dfrac{a_2}{h_3^3}}, \\
D_{12}^0 &= D_{21}^0 = \nu D_{22}^0, \\
D_{66}^0 &= \frac{1-\nu}{2} D_{22}^0 = \frac{E}{24\left(1+\nu\right)}\frac{a}{\dfrac{a_1}{h_1^3}+\dfrac{a_2}{h_3^3}}.
\end{aligned}
\tag{4.22}
$$

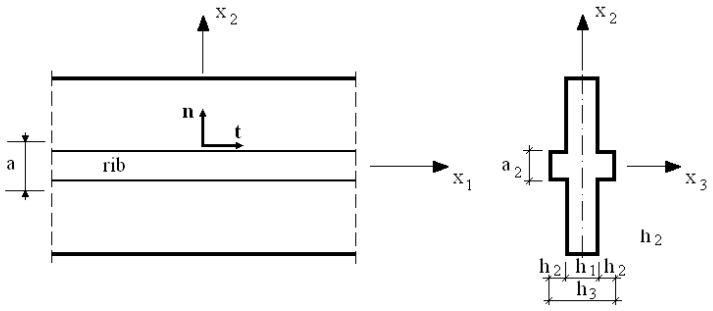

Fig. 7. Geometry of the plate structure reinforced by the rib

Consider now the functional of curvatures and displacements (4.10) and choose the width of the rib a_2 as the topological parameter. The topological derivative should be calculated at the value $a_2 = 0$. Thus, using the adjoint structure method, specified by (4.11), the topological derivative takes the form (cf. [4])

$$
\left.\frac{\partial G}{\partial a_2}\right|_{a_2=0} = a\int_l \left(\left.\frac{\partial F}{\partial a_2}\right|_{a_2=0} - \boldsymbol{\kappa}^T \left.\frac{\partial \mathbf{D}^0}{\partial a_2}\right|_{a_2=0} \boldsymbol{\kappa}^a \right) dl \,. \tag{4.23}
$$

The particular components of the stiffness matrix $\mathbf{D}^0$ are expressed by (4.22). Taking into account that derivatives of these components can be determined in the form

$$\left.\frac{\partial D_{11}^0}{\partial a_2}\right|_{a_2=0} = \frac{E}{12a\left(1-\nu^2\right)}\left(h_3^3-h_1^3\right)\left(1-\nu^2+\frac{h_1^3}{h_3^3}\nu^2\right),$$
$$\left.\frac{\partial D_{22}^0}{\partial a_2}\right|_{a_2=0} = \frac{E}{12a\left(1-\nu^2\right)}\left(h_3^3-h_1^3\right)\frac{h_1^3}{h_3^3},$$
$$\left.\frac{\partial D_{12}^0}{\partial a_2}\right|_{a_2=0} = \nu\left.\frac{\partial D_{22}^0}{\partial a_2}\right|_{a_2=0}, \tag{4.24}$$
$$\left.\frac{\partial D_{66}^0}{\partial a_2}\right|_{a_2=0} = \frac{1-\nu}{2}\left.\frac{\partial D_{22}^0}{\partial a_2}\right|_{a_2=0},$$

the topological derivative is presented by the formula

$$\left.\frac{\partial G}{\partial a_2}\right|_{a_2=0} = \int_l \left[a\left.\frac{\partial F}{\partial a_2}\right|_{a_2=0} - D_r\left(1-\nu^2+\frac{h_1^3}{h_3^3}\nu^2\right)\kappa_{11}\kappa_{11}^a - D_r\frac{h_1^3}{h_3^3}\kappa_{22}\kappa_{22}^a + \right.$$
$$\left. -\nu D_r\frac{h_1^3}{h_3^3}\left(\kappa_{11}\kappa_{22}^a+\kappa_{22}\kappa_{11}^a\right) - D_r\frac{1-\nu}{2}\frac{h_1^3}{h_3^3}\kappa_{12}\kappa_{12}^a\right] dl, \tag{4.25}$$

where $D_r = \dfrac{E}{12\left(1-\nu^2\right)}\left(h_3^3-h_1^3\right)$.

The formulas for the topological derivatives of cost functionals and the functionals of stresses and reactions can be found in [4].

4.4. Example: reinforcement of plate by ribs

The rectangular plate (3000mm×2000mm) shown in Fig. 8a has been analyzed (cf. [4]). The structure is made of steel (the Young's modulus is E = $2.05\cdot10^5$ MPa and the Poisson's ratio is $\nu = 0.3$). Its initial thickness is 15 mm. The plate is clamped on three edges, while fourth (upper) edge is free. Transverse load varies linearly along the height of the plate.

Here, the optimization problem (4.1) corresponds to the minimization of the strain energy of the structure with a constraint imposed on the total volume of the plate, where C_0 corresponds to the initial volume. Also, geometrical constraints limiting the minimum distance between the non-intersecting ribs to 200 mm and the minimum thickness of the plate to 10 mm, have been used (cf. [4]).

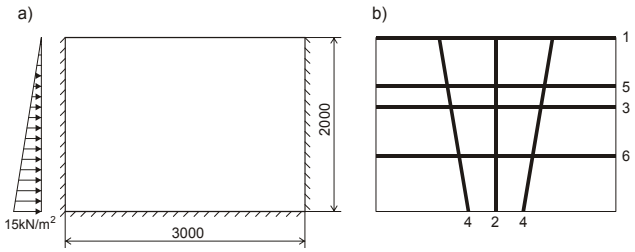

Fig. 8. Optimal design of plate reinforced by ribs: a) geometry of the plate, b) optimal layout of ribs

Rectilinear ribs of cross-sectional dimensions: width a_2 = 50 mm, total height h_3 = 40 mm, have been introduced into positions, which are specified from the solution of the problem of the initial localization. In the first stage, seven ribs are introduced, and next, slight correction of their position is performed. The constraint imposed on the minimum thickness of the plate is active. Fig. 8b shows the layout of the ribs and the order of their introduction. The ratio of the strain energies of the initial and optimal designs is $U^{(init)} / U^{(opt)} = 2.354$.

5. CONCLUDING REMARKS

The application of topological derivative in material science and optimal design has been discussed in the paper. Finite topology modification approach based on topological derivative has been formulated in particular. In the case of material science, topological derivative is used to describe the process of nucleation and growth of new phases and the process of crack nucleation. In the case of optimal design, approaches based on topological derivative are applied in the problems of topology and shape optimization and the problems of reinforcement optimization for disk and plate structures.

Examples shown in the paper confirm the applicability and usefulness of the topological derivative approach. It is noticed, that, usually, the application of the finite modifications essentially reduces computation time required for the generation of improved or optimal designs.

ACKNOWLEDGEMENTS

The work was partially supported by the Polish State Committee for Scientific Research (KBN); grant no. 4T07E 023 28.

BIBLIOGRAPHY

1. Allaire G.: Shape optimization by the homogenization method, New York, Springer 2002.
2. Bendsoe M.P.: Optimization of structural topology, shape and material, Berlin, Springer1997.
3. Bendsoe M.P., Kikuchi N.: Generating optimal topologies in structural design using a homogenization method, Comp. Meth. Appl. Mech. Eng., **71** (1988), 197-224.
4. Bojczuk D.: Method of optimal reinforcement of structures based on topological derivative, in: Proc. III Europ. Conf. Comp. Mech., C. Mota Soares et al. (Eds), Lisbon, Springer 2006, on CD.
5. Bojczuk D., Mróz Z.: On optimal design of supports in beam and frame structures, Struct. Optim., **16** (1998), 47-57.
6. Bojczuk D., Mróz Z.: Optimal design of trusses with account for topology variation, Mech. Struct. Mach., **26** (1998), 21-40.
7. Bojczuk D., Mróz Z.: Optimal topology and configuration design of trusses with stress and buckling constraints, Struct. Optim., **17** (1999), 25-35.
8. Bojczuk D., Szteleblak W.: Application of finite variations to topology and shape optimization of 2D structures, J. Theoret. Appl. Mech., **44** (2006), 323-349.
9. Burczyński T., Kokot G.: Evolutionary algorithms and boundary element method in generalized shape optimization, J. Theor. Appl. Mech., **41** (2003), 341-364.
10. Cherkaev A.V.: Variational methods for structural optimization, New York, Springer 2000.
11. Dems K., Mróz Z.: Variational approach by means of adjoint systems to structural optimization and sensitivity analysis. II. Structure shape variation, Int. J. Solids Struct., **19** (1984), 527-552.
12. Dems K., Mróz, Z.: Optimal design of rib-stiffeners in disks and plates, Int. J. Solids Struct., **25** (1989), 973-998.
13. Eschenauer H.A., Kobelev V.V., Schumacher A.: Bubble method for topology and shape optimization of structures, Struct. Optim., **8** (1994), 42-51.
14. Garstecki A., Mróz Z.: Optimal design of supports of elastic structures subjected to loads and initial distortions, Mech. Struct. Mach., **15** (1987), 47-68.
15. Hills R.E., Abbaschian R.: Physical metallurgy principles, PWS Publ. Co. 1994.
16. Kirsch U.: Optimal topologies of structures, Appl. Mech. Rev., **42** (1989), 223-239.
17. Lam Y.C., Santhikumar S.: Automated rib location and optimization for plate structures, Struct. Multidisc. Optim., **25** (2003), 35-45.

18. Lewiński T., Telega J.J.: Plates, laminates and shells. Asymptotic analysis and homogenization, Singapore, World Scientific 2000.
19. Mróz Z., Bojczuk D.: Topological derivative and its application in optimal design of truss and beam structures for displacement, stress and buckling constraints, in: Topology Optimization of Structures and Composite Continua, G. I. N. Rozvany, N. Olhof N. (Eds.), Kluwer Ac. Publ. 2000, 91-105.
20. Mróz Z., Bojczuk D.: Finite topology variation in optimal design of structures, Struct. Multidisc. Optim., **25** (2003), 153-173.
21. Mróz Z., Garstecki A.: Optimal loading conditions in the design and identification of structures. Part 1: discrete formulation, Struct. Multidisc. Optim., **29** (2005), 1-18.
22. Petryk H., Mróz Z.: Time derivatives of integrals and functionals defined on varying volume and surface domains, Arch. Mech., **38** (1986), 697-724.
23. Sethian J.A.: Level set methods and fast marching methods: evolving interfaces in computational geometry, Fluid Mechanics Computer Vision and Materials Science, Cambr. Univ. Press 1999.
24. Sokolowski J., Żochowski T.: On topological derivative in shape optimization, SIAM J. Control Optim., **37** (1999), 1251-1272.
25. Wang X., Wang M.Y., Guo D.: Structural shape and topology optimization in a level-set-based framework of region representation, Struct. Multidisc. Optim., **27** (2004), 1-19
26. Xia Q., Wang M.Y., Wang S., Chen S.: Semi-Lagrange method for level-set based structural topology and shape optimization, Struct. Multidisc. Optim., **32** (2006), in print.
27. Xie Y.M., Steven G.P.: A simple evolutionary procedure for structural optimization, Comp. Struct., **49** (1993), 885-896.

Dedicated to Professor Andrzej Garstecki with best wishes for his 70-th birthday